



OPEN

# Chains of Carbon Nanotetrahedra/ Nanoribbons

Hideo Kohno<sup>1</sup> & Takayuki Hasegawa<sup>2</sup>

SUBJECT AREAS:

CARBON NANOTUBES  
AND FULLERENES

NANOSCALE MATERIALS

Received

4 September 2014

Accepted

19 January 2015

Published

12 February 2015

Correspondence and  
requests for materials  
should be addressed to  
H.K. (kohno.hideo@  
kochi-tech.ac.jp)

<sup>1</sup>School of Environmental Science and Engineering, Kochi University of Technology, Tosayamada, Kami, Kochi 782-8502 Japan,  
<sup>2</sup>Graduate School of Science, Osaka University, 1-1 Machikaneyama, Toyonaka Osaka 560-0043, Japan.

**Flattening of a carbon nanotube results in the formation of a carbon nanoribbon with well-defined edges. In addition, a switching of the flattening direction by about a right angle yields a carbon nanotetrahedron at the switching point in a nanoribbon. Here, we report that chains of carbon nanotetrahedra/nanoribbons are formed via sequential switching of the flattening direction of multiwalled carbon nanotubes, in which neighboring two nanotetrahedra are connected by a short nanoribbon, namely a flattened nanotube. We suggest that the formation of nanotetrahedra chains is caused by a quasi-periodic instability of catalyst iron nanoparticles during the chemical vapor deposition growth. In addition, two adjoining carbon nanotetrahedra were found.**

**F**abrication of graphene<sup>1</sup> nanoribbons from carbon nanotubes (CNTs)<sup>2</sup> is promising, since the width and thickness of the nanoribbons can easily be adjusted by using carbon nanotubes with appropriate diameters and number of walls. As carbon nanotube growth technology is well established, this approach is useful for fabricating graphene nanoribbons with the desired bandgap opening<sup>3</sup>. Two types of methods have been developed so far to fabricate graphene/graphite nanoribbons from carbon nanotubes: unzipping<sup>4–8</sup> and collapsing<sup>9–13</sup>. The former has the potential to yield monolayer graphene nanoribbons, although the edge quality of nanoribbons fabricated using this method is low and difficult to control. The latter method is incapable of forming monolayer graphene nanoribbons (the thinnest obtainable by this method are bilayers), however, the edges of graphene nanoribbons grown by this method can easily be defect free. It is known that the larger a carbon nanotube's diameter and the thinner its wall, the more stable it is when it flattens to form a nanoribbon, however, the flattening mechanism has yet to be determined. In our previous study, we have proposed a mechanism for nanotube flattening: a  $\gamma$ -Fe catalyst nanoparticle expels a carbon nanotube, forcing the nanotube to flatten<sup>14</sup>. We have observed that in addition to carbon nanoribbons, carbon nanotetrahedra were formed: When the flattening direction switches by about a right angle during nanoribbon growth, a nanotetrahedron is formed at the switching point. In the present paper, we report briefly on the formation of chains of carbon nanotetrahedra, in which the nanotetrahedra are connected by nanoribbons, which is caused by sequential changes in the flattening direction that occur during nanoribbon (flattened nanotube) growth. The structure of the chains of nanotetrahedra/nanoribbons is revealed through electron microscopy. Formation of one or two nanotetrahedra in a flattened CNT which was reported in our previous paper could be by coincidence; however, the sequential formation of several nanotetrahedra, namely sequential changes in the flattening direction, must be an inevitable phenomenon under a certain condition. Therefore, the difference in the number of nanotetrahedra in a flattened CNT is not just quantitative, but is essentially qualitative. This makes this paper definitively different from the previous paper.

## Results and discussion

We found some chains of carbon nanotetrahedra/nanoribbons in addition to CNTs, carbon nanoribbons, and nanotetrahedron/nanoribbon structures in the products (relative fractions: chains 33%, tubes 36%, tube/ribbon structures 21%, ribbons 9%, and others 1%, based on the sampling of 798 carbon nanostructures). SEM images of chains of carbon nanotetrahedron/nanoribbon structures are shown in Fig. 1 along with a schematic three-dimensional model. Several chains of carbon nanotetrahedra/nanoribbons can be seen in the SEM image in Fig. 1(a). The enlarged SEM image (Fig. 1(b)) clearly shows that the structure is not formed by twisting the nanoribbon<sup>15–17</sup>. Twisting of a nanoribbon is caused by continuous and gradual rotation of the flattening direction, and the twisted nanoribbon has a periodic structure as a result of the rotation. When viewed along a direction normal to its growth direction, the flat plane of the nanoribbon becomes parallel to the viewing direction periodically as shown in Fig. 3 of Ref. 17. A twisted nanoribbon is collapsed thoroughly from one end to another,

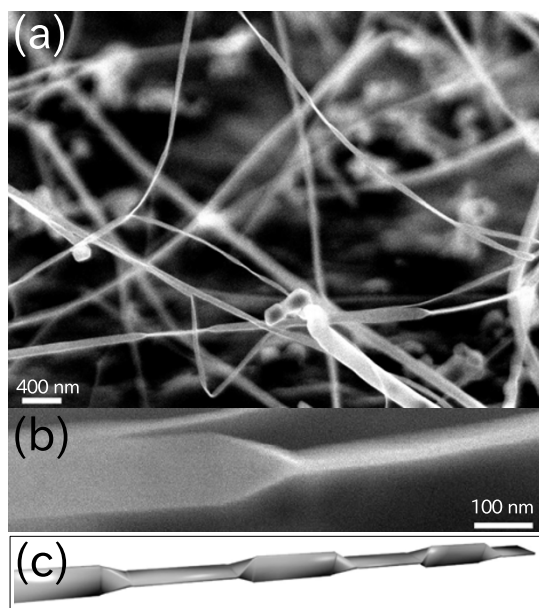
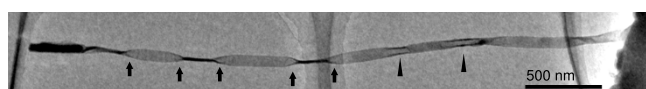


**Figure 1** | (a) SEM image of chains of carbon nanotetrahedra/nanoribbons. (b) Enlarged SEM image of a carbon nanotetrahedron. (c) Three-dimensional schematic model of a chain of carbon nanotetrahedra/nanoribbons.

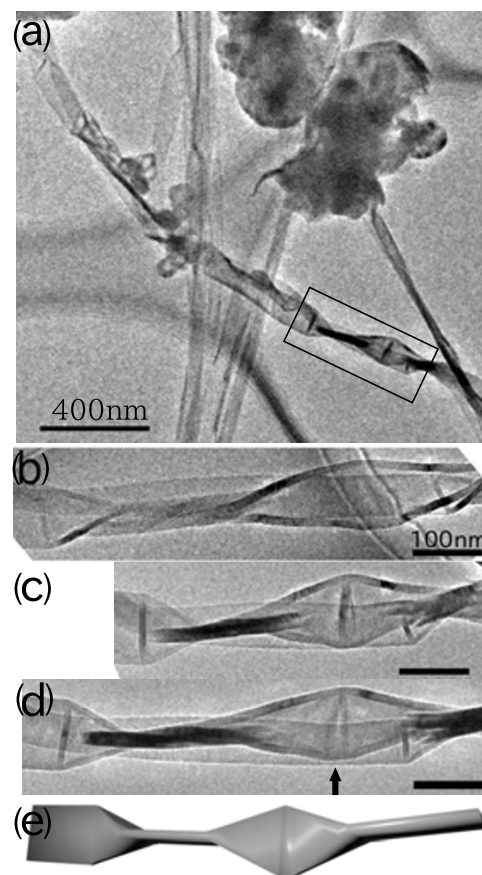
and no tetrahedron is formed in it by such twisting. We emphasize that our chains of tetrahedra/ribbons are different from twisted nanoribbons. The distance between adjoining nanotetrahedra was about 200–1000 nm, with a nanoribbon width of around 50 nm. High-resolution TEM revealed that the number of walls of the original carbon nanotubes was around 10–30.

Fig. 2 shows a TEM image of a chain. Five nanotetrahedra (indicated by arrows) are located near the tip of the nanoribbon. In addition to these nanotetrahedra, the TEM image shows another marked feature: two sections (indicated by arrowheads) show clearer edges than the parts of nanoribbon. This suggests that these two sections have a tubular form. Since the Fe catalyst nanoparticle is located to the left in the figure, it can be concluded that the tubular parts were formed first, then the nanotetrahedra were formed. Fig. 2 suggests that a fluctuation occurred around the tubular parts, however, the force exerted to flatten the tube was not strong enough in one direction which was normal to the TEM observation in Fig. 2, where the flattening ‘direction’ is defined as the direction normal to the nanoribbon’s wide surface. Then, the intensity of the fluctuation became strong enough to force the nanotube to flatten both normal and parallel to the viewing direction, resulting in the formation of the five nanotetrahedra. In addition, Fig. 2 also shows that nanoribbons with a flattening direction parallel to the viewing direction are longer than those flattened in the direction normal to the viewing direction. This suggests that the flattening force was different along these two directions, presumably owing to the initially asymmetrical shape of the catalyst nanoparticle.

In addition to the quasiperiodic arrangement of nanotetrahedra, we also found two adjoining nanotetrahedra (see Fig. 3). A third nanotetrahedron was located about 200 nm away from these two nanotetrahedra. As seen in Fig. 3, the two adjoining nanotetrahedra



**Figure 2** | TEM image of a chain of carbon nanotetrahedra/nanoribbons. The arrows and arrowheads indicate tetrahedra and parts of the tube, respectively.



**Figure 3** | (a) TEM image of a nanoribbon with two adjoining nanotetrahedra. (b)–(d) Enlarged images viewed along different directions. (e) Schematic 3D model of the nanoribbon with adjoining nanotetrahedra.

share their top apexes at the junction, while there seems to be a short distance of about 40 nm between their apexes at the bottom, judging from the triangle in the TEM images in Figs. 3(c) and (d), indicated by the arrow. If a defect-free MWCNT flattens to form adjoining nanotetrahedra, it would be very unstable, since a large energy is necessary to form the shape, while the gain owing to the van der Waals force is limited. Therefore, the formation of adjoining nanotetrahedra strongly suggests that some structural defects are induced during growth and that this structure is formed immediately after a MWCNT is expelled from its metal catalyst nanoparticle.

It is known that CNTs with diameter smaller than a certain critical value can not become flattened due to large elastic energy required for flattening, and that flattened CNTs become unstable with increasing the number of walls<sup>18</sup>. It is obvious that switching the flattening direction gives further increase in elastic energy in comparison with simple one direction flattening. It is also known that defects in CNTs affect the flattening of CNTs. Ling et al.<sup>19</sup> reported in their theoretical study that Stone-Wales defects stabilize flattening of armchair SWCNTs, while the defects inhibit the flattening of zigzag SWCNTs. Choi et al.<sup>20</sup> investigated flattening of MWCNTs by sonication experimentally and found that defective MWCNTs did not become flattened even after longtime sonication to the contrary, in which they did not identify the structure of defects. These reports suggest that defects in CNTs work in various way on flattening. It would be possible that some kind of mechanical instability works to form a chain of nanotetrahedra with relatively long interval between nanotetrahedra after a CNT is formed initially with the fully tubular form; however, mechanical instability would not result in the forma-

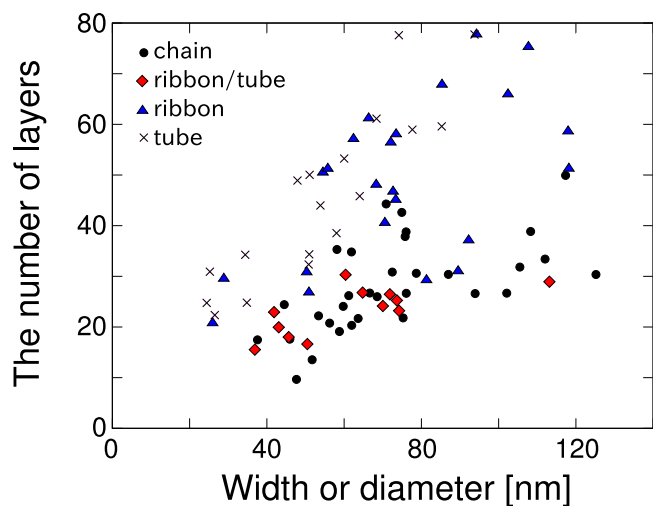


**Figure 4** | Width (diameter)-the number of layers plot of chains, ribbon/tube structures, ribbons, and tubes.

tion of the adjoining nanotetrahedra shown in Fig. 3. Our finding of the adjoining nanotetrahedra suggests that mechanical instability of CNTs would not be a dominant contribution to the formation of the chains of nanotetrahedra, especially the adjoining nanotetrahedra.

In order to obtain further insight into understanding the chain formation, we measured how the number of layers and width (diameter) of CNTs affect the chain formation and flattening as shown in Fig. 4. In the number of layer-width space, the distributions of chains and ribbon/tube structures overlaps each other, and there is a tendency that chains and ribbon/tube structures have less number of layers and/or a larger width than ribbons and tubes. Ribbons distribute widely, but it seems that they have a tendency to have less number of layers and/or a larger width than tubes. When increasing the number of layers and/or decreasing the diameter, tubes are most stable, then simple ribbons, and lastly tube/ribbon structures and chains. It is reasonable that a ribbon-tube junction requires some energy comparable to that for the formation of a tetrahedron since there is large strain in such a junction, a local structure. However, a tetrahedral junction would require larger energy than a ribbon-tube junction since the local strain is larger in a tetrahedral junction. The fact that the distributions of chains and ribbon/tube structures are almost the same suggests that some defects in the junctions stabilize the junctions.

We previously reported the formation of Si nanochains, in which Si nanoparticles are periodically connected with oxide nanowires and alternately in one dimension<sup>21</sup>. It was concluded that the Si nanochain formation was induced by a periodic modulation in diameter and surface oxidation during the growth of Si nanowires<sup>22,23</sup>. We speculate that the formation of the chains of carbon nanotetrahedra/nanoribbons was induced by some kind of quasiperiodic instability of the Fe catalyst nanoparticles during the growth, such as instability of their shape, resulting in the quasiperiodic switching in the flattening direction.

In summary, we have found chains of carbon nanotetrahedra/nanoribbons accompanying the simple metal nanoparticle-mediated chemical vapor deposition growth of CNTs. Quasiperiodic switching in the direction of nanotube flattening resulted in chain formation. The structure of these chains was revealed by SEM and TEM observations. For further study, such as optical or electrical measurements, it is necessary to develop a high-yield growth method for the chains. This may also enable control over chain dimensions. In addition, *in-situ* TEM observation of the chain growth process<sup>24</sup> would elucidate the formation mechanism.

## Methods

The growth procedure was as follows. First, a 20-nm-thick Fe layer was deposited on a SiO<sub>2</sub> substrate. Then, this sample was sealed in an evacuated silica tube (inner diameter = 6 mm, length ≈ 11.5 cm) with 0.5 mg of hexadecanoic acid [C<sub>15</sub>H<sub>31</sub>C(=O)OH] as a carbon source. The sample was heated at 1000°C for 30 min, then cooled to room temperature after growth. The grown carbon nanostructures were mounted on a carbon microgrid for transmission electron microscopy (TEM) and scanning electron microscopy (SEM). A JEOL JEM-2010 TEM system (operated at 160 kV), an FEI TecnaiG2-20 TEM system (operated at 200 kV), and a JSM-7300F SEM system (operated at 5 kV) were used for the observations.

- Novoselov, K. S. *et al.* Electric field effect in atomically thin carbon films. *Science* **306**, 666–669 (2004).
- Iijima, S. Helical microtubules of graphitic carbon. *Nature* **354**, 56–58 (1991).
- Han, M. Y., Özyilmaz, B., Zhang, Y. & Kim, P. Energy band-gap engineering of graphene nanoribbons. *Phys. Rev. Lett.* **98**, 206805 (2007).
- Kosynkin, D. V. *et al.* Longitudinal unzipping of carbon nanotubes to form graphene nanoribbons. *Nature* **458**, 872–877 (2009).
- Jiao, L., Zhang, L., Wang, X., Diankov, G. & Dai, H. Narrow graphene nanoribbons from carbon nanotubes. *Nature* **458**, 877–880 (2009).
- Cano-Márquez, A. G. *et al.* Graphene Sheets and Ribbons Produced by Lithium Intercalation and Exfoliation of Carbon Nanotubes. *Nano Letters* **9**, 1527–1533 (2009).
- Elias, A. L. *et al.* Longitudinal Cutting of Pure and Doped Carbon Nanotubes to Form Graphitic Nanoribbons Using Metal Clusters as Nanoscalpels. *Nano Letters* **10**, 366–372 (2010).
- Kim, K., Sussman, A. & Zettl, A. Graphene Nanoribbons Obtained by Electrically Unwrapping Carbon Nanotubes. *ACS Nano* **4**, 1362–1366 (2010).
- Chopra, N. G. *et al.* A Fully collapsed carbon nanotubes. *Nature* **377**, 135–138 (1995).
- Gutiérrez, N. G. *et al.* Thermal conversion of bundles carbon nanotubes into graphitic ribbons. *Nano Letters* **5**, 2195–2201 (2005).
- Lin, C.-T., Chen, T.-H., Chin, T.-S., Lee, C.-Y. & Chiu, H.-T. Quasi two-dimensional carbon nanobelts synthesized using a template method. *Carbon* **46**, 741–746 (2008).
- Gao, G. H., Cagin, T. & Goddard, W. A. Energetics, structure, mechanical and vibrational properties of single-walled carbon nanotubes. *Nanotechnology* **9**, 184–191 (1998).
- Tang, T., Jagota, A., Hui, C. Y. & Glassmaker, N. J. Adhesion between single-walled carbon nanotubes. *J. Appl. Phys.* **97**, 074310 (2005).
- Kohno, H., Komine, T., Hasegawa, T., Niioka, H. & Ichikawa, S. Formation of a carbon nanoribbon by spontaneous collapse of a carbon nanotube grown from a  $\gamma$ -Fe nanoparticle via an origami mechanism. *Nanoscale* **5**, 570–573 (2013).
- Yu, M.-F., Dyer, M. J. & Ruoff, R. S. Structure and mechanical flexibility of carbon nanotube ribbons: an atomic-force microscopy study. *J. Appl. Phys.* **89**, 4554–4557 (2001).
- Yu, M.-F., Kowalewski, T. & Ruoff, R. S. Structural analysis of collapsed, and twisted and collapsed, multiwalled carbon nanotubes by atomic force microscopy. *Phys. Rev. Lett.* **86**, 87–90 (2001).
- Yu, M.-F. *et al.* Locked twist in multiwalled carbon-nanotube ribbons. *Phys. Rev. B* **64**, 241403(R) (2001).
- Zhang, S. *et al.* Transition states and minimum energy pathways for collapse of carbon nanotubes. *Phys. Rev. B* **73**, 075423 (2006).
- Ling, C.-C., Xue, Q.-Z., Chu, L.-Y., Jing, N.-N. & Zhou, X.-Y. Radial collapse of carbon nanotubes without and with Stone-Wales defects under hydrostatic pressure. *RSC Advances* **2**, 12182–12189 (2012).
- Choi, D. H. *et al.* Fabrication and characterization of fully flattened carbon nanotubes: a new graphene nanoribbon analogue. *Sci. Rep.* **3**, 1617 (2013).
- Kohno, H. & Takeda, S. Self-organized chain of crystalline-silicon nanospheres. *Appl. Phys. Lett.* **73**, 3144–3146 (1998).
- Kohno, H. & Takeda, S. Periodic instability in growth of chains of crystalline-silicon nanospheres. *J. Cryst. Growth* **216**, 185–191 (2000).
- Kohno, H., Takeda, S. & Tanaka, K. Plasmon-loss imaging of chains of crystalline-silicon nanospheres and silicon nanowires. *J. Electron Microsc.* **49**, 275–280 (2000).
- Yoshida, H. *et al.* Atomic-scale in-situ observation of carbon nanotube growth from solid state iron carbide nanoparticles. *Nano Lett.* **8**, 2082–2086 (2008).

## Acknowledgments

This work was supported in part by Adaptable and Seamless Technology Transfer Program through target-driven R&D, Japan Science and Technology Agency. The authors thank Y. Masuda, S. Ichikawa, N. Nitta, and H. Furuta for their support.

## Author contributions

H.K. designed the project and wrote the manuscript. T.H. fabricated the materials, carried out the transmission electron microscopy observations, and prepared the figures.



## Additional information

**Competing financial interests:** The authors declare no competing financial interests.

**How to cite this article:** Kohno, H. & Hasegawa, T. Chains of Carbon Nanotrahedra/Nanoribbons. *Sci. Rep.* 5, 8430; DOI:10.1038/srep08430 (2015).



This work is licensed under a Creative Commons Attribution-NonCommercial-ShareAlike 4.0 International License. The images or other third party material in this article are included in the article's Creative Commons license, unless indicated otherwise in the credit line; if the material is not included under the Creative Commons license, users will need to obtain permission from the license holder in order to reproduce the material. To view a copy of this license, visit <http://creativecommons.org/licenses/by-nc-sa/4.0/>